Deep Learning for Segmentation, Detection and Classification of Prostate Cancer Using mp-MRI

Tapan Dandawala
Department of Computer Science, The University of Western Ontario
{tdandawa@uwo.ca}

Abstract*—Prostate cancer is one of the most common cancers in men and early detection is essential for successful treatment. Multiparametric Magnetic resonance imaging (mp-MRI) is a powerful imaging modality for prostate cancer detection. However, manual segmentation and classification of prostate cancer lesions from MRI images is a time-consuming and labor-intensive task. In this study, we use Deep Learning methods (CNN) that takes mp-MRI scans to perform prostate segmentation, lesion detection and lesion classification into their significance i.e., significant, and non-significant which will provide insights to doctors which help them to perform diagnosis with better accuracy

Keywords*— mp-MRI, Prostate Cancer Detection, segmentation, CNN, deep learning, detection

1. Introduction

Prostate cancer (PCa) is the most common type of cancer among men in the United States, with an estimated 268,490 new cases and 34,500 deaths in 2022 alone [32]. It is a serious health concern for men of all ages and races. The good news is that early detection and treatment can significantly improve the chances of survival. Computer-aided diagnosis (CAD) has become an important tool for early detection and diagnosis of PCa. CAD systems are computer-based systems that use algorithms to analyze medical images such as ultrasound, MRI, or CT scans to detect abnormalities or suspicious areas in the prostate gland. This article will provide an overview of PCa, its risk factors, current screening methods, and how CAD can be used to improve early detection and diagnosis of PCa. The article will also compare different studies.

1.1 What is Prostate Cancer?

PCa is a type of malignant tumor that develops in the prostate gland, which is a small walnut-sized organ located just below the bladder in men. It produces seminal fluid which helps nourish and transport sperm during ejaculation. PCa occurs when abnormal cells grow uncontrollably in the prostate gland. These cells can spread to other parts of the body if left untreated.

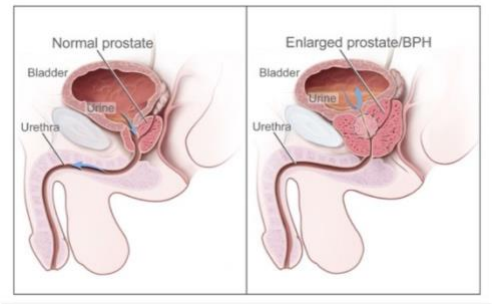

Figure 1: Cross-section of Prostate with PCa and No PCa [33]

1.1.1 Risk Factors for Prostate Cancer

There are several risk factors associated with developing PCa including age (over 65), family history (having a father or brother with PCa), race (African American men are at higher risk than other races), diet (high fat diets may increase risk), obesity (being overweight increases risk), smoking

(smoking increases risk), and certain medications (long-term use of certain medications may increase risk) [34].

1.1.2 Screening & Grading for Prostate Cancer

Screening tests are used to detect diseases before symptoms appear. For PCa, two tests are commonly used: digital rectal exam (DRE) and prostate specific antigen test (PSA). During a DRE, a doctor inserts a gloved finger into the rectum to feel for any abnormalities in the size or shape of the prostate gland. The PSA test measures levels of PSA in blood samples; elevated levels may indicate an increased risk for developing PCa. However, both tests have limitations; DREs can miss some cancers while PSA tests can produce false positives due to other conditions such as benign prostatic hyperplasia or prostatitis.

MRI of the prostate has become a more frequent practice in radiology and is usually done as either a multi-parametric (mp-MRI) or bi-parametric (bi-MRI). This has enabled doctors and radiologists to detect, assess, and analyze PCa based on the images. To help with this process, an internationally recognized system called PI-RADS (Prostate Imaging-Reporting and Data System) was created by the American College of Radiology [36], AdMeTech Foundation, and ESUR. Its purpose is to develop a scoring system that can detect clinically relevant PCa early on and reduce unnecessary biopsies for benign or subclinical diseases. However, mistakes in detection or interpretation still occur during diagnosis.

These errors are caused by many factors such as observer limitations like fatigue or distraction; lack of clinical experience; image quality; complexity of cases; imbalanced data; overlapping structures in MRIs; and large amounts of data which can be time consuming [35].

The Gleason Grading System or Grade (GGG) [33] is a commonly used metric to measure the progression of PCa. It is based on the analysis of biopsy samples, which are studied to determine the aggressiveness of the cancerous cells. The grade is assigned on a scale from 1 to 5, with 1 and 2 indicating no cancerous tissue was detected, 3 suggesting a slow-growing tumor, and 5 indicating a highly aggressive form of PCa. The two most common grades observed in biopsy samples are then combined (3 + 4 = 7) to get a final score. This score helps doctors evaluate how dangerous the cancer is and will influence treatment decisions.

2. Related Work

Numerous studies have been conducted to create a machine learning model that could assist physicians in diagnosing prostate cancer. These computer-aided diagnosis (CAD) systems typically aim to achieve different objectives, such as segmenting the prostate and estimating its volume, as well as predicting the aggressiveness

2.1 Prostate Segmentation & Size Estimation

Prostate segmentation is the process of identifying and delineating the prostate gland in medical images. It is an important step in the diagnosis and treatment of prostate cancer, as it allows for the accurate measurement of the size and shape of the prostate. Prostate segmentation can be performed manually or automatically using a variety of techniques, including region-based segmentation, active contours, and deep learning. The accuracy of the segmentation is dependent on the quality of the input images and the chosen technique.

A Traditional Machine Learning Technique of using fuzzy c-means clustering, categorize data into groups via unsupervised learning was used by Rundo et al. [1] to perform segmentation on T1W and T2W mpMRI Images. It was evaluated on 21

patients to get a Dice Score of 0.91. A dice score in Machine Learning is a metric used to evaluate the performance of a model in segmentation tasks. It is calculated by taking the ratio of the number of pixels correctly classified to the total number of pixels in an image. The dice score ranges from 0 to 1, with 1 being a perfect score. Dice Score of 0.91 demonstrate that segmentation of prostate is done with high accuracy and precision.

In addition to fuzzy c-means clustering, deep learning has been widely used for full prostate segmentation since they accomplish feature extraction independently. This was spurred by the PROMISE12 [25] challenge dataset, which contained 100 patients, and was released in 2012. Two research groups, Tian et al. [2] and Karimi et al. [3], both employed convolutional neural networks (CNNs). Tian et al. [2] trained their CNN on T2-weighted mpMRI images from 140 patients and achieved a Dice score of 0.85. Karimi et al.'s [3] CNN was trained on a limited dataset of 49 T2-weighted mpMRI images with data augmentation, and they achieved a Dice score of 0.88. These studies showed that prostate segmentation can be accomplished with commonly used technical designs, as evidenced by their high Dice scores [4].

According to a study done by Michelle D et al. [4], the use of a special algorithm, U-Net, was compared. U-Net has been proposed as a method for fully automated prostate segmentation and volume estimation [5]. This algorithm compresses an image, extracts features during the compression process, and classifies each pixel in the image [5]. Three studies that used U-Net for prostate segmentation achieved Dice scores of 0.89, 0.93, and 0.89 [6-8], indicating that U-Net can effectively segment the prostate with datasets ranging from 81 to 163 patients. The high Dice scores across multiple studies with similar network architectures demonstrate considerable progress towards completely automated prostate segmentation and volume approximation.

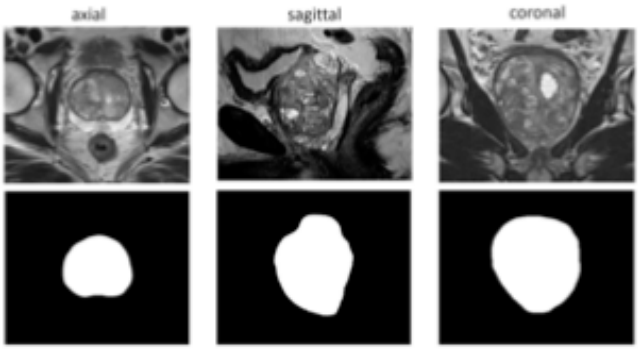

Figure 2: Different mp-MRI modalities with their Prostate segmentation [37].

2.2 Prostate Lesion: Segmentation, Detection

Once the prostate has been identified by a computer or physician, the next step is to identify any areas of the gland that could be potentially Ca. These regions are referred to as 'lesions'. A prostatic lesion is an abnormal growth of cells that may or may not be cancerous. Identifying these areas of interest will not only be beneficial for determining if the lesions are cancerous or not, but it can also help the doctor visualize any abnormal zones in the prostate and aid in diagnosis. As discussed above the doctors can make mistakes in identifying these lesions for a variety of reasons. ML approaches have been used to identify Potential Malignant Lesions independently and automatically.

With CNNs promising results in the computer-vision field, the medical image research community has shifted their focus to deep learning for cancer detection. Most of the proposed algorithms require user-drawn regions of interest (ROI) to classify as PCa lesions or non-PCa lesions. Lay et al. [12] used a prostate computer-aided diagnosis (CAD) based on a random forest for prostate lesion detection

(Table 2). The method uses a combination of spatial, intensity, and texture features extracted from mp-MRI sequences. This study's dataset used 224 patient cases across three sequences (T2-weighted, ADC, and DWI) for a total of 287 benign lesions and 123 lesions with a Gleason score of 6 or higher [12]. Lay et al.'s random forest technique yielded an area under the curve (AUC) score of 0.93. Xu et al. [13] implemented a type of neural network with extensive layers, ResNet [14]. This study used images from the Cancer Imaging Archive data portal i.e., ProstateX and ProstateX2. They achieved an AUC of 0.97.

Tsehay et al. [15] conducted a 3 x 3-pixel level analysis by 5 convolution layers deep VGGNet [18] inspired CNNs with 196 patients. They fine-tuned their classifier by cross-validation method within the training set with 144 patients and achieved area under ROC curve (AUC) of 0.90 AUC on a separated test set of 52 patients. The result was based on 3 x 3 windows of pixels extracted from MRI slices of DWI, T2-weighted images (T2w), and b-value images of 2000s mm2.

Le et al. [16] conducted two-dimensional (2D) ROI classification with combination of fused multimodal Residual Network (ResNet) [14] and the traditional handcrafted feature extraction method. They augmented the training dataset and used the test set for fine-tuning and evaluating their classifier. They achieved ROI-level (lesion-level) AUC of 0.91. Liu et al. [17] used VGGNet inspired 2D CNNs classifier to classify each sample corresponding to a 32 x 32 ROI (lesion) centered around biopsy location using a dataset, which was part of ProstateX challenge competition ("SPIE-AAPM-NCI Prostate MR Classification Challenge") [19]. They separated the dataset, 341 patients, into 3 sets, the training set with 199 patients for training, validation set with 30 patients for fine-tuning, and test set with 107 patients for evaluation, and applied data augmentation to all 3 sets. They used 4 different types of inputs which were generated with different combinations of DWI, apparent diffusion coefficient map (ADC), Ktrans, and T2w for their study. They achieved AUC of 0.84 with the augmented test data.

Mehrtash et al. [20] also used VGGNet inspired 9 convolution layers deep three dimensional (3D) CNNs classifier to classify 3D PCa lesions vs. non PCa lesions with 32 x 32 x 12 ROI using ADC, high b-value images, and Ktrans from dynamic contrast enhanced magnetic resonance imaging (DCE-MRI) of ProstateX challenge dataset [19]. They separated the data set with 341 patients into training set with 201 patients and test set with 140 patients and achieved lesion-level performance of 0.80 AUC on their test set. They applied cross-validation method within the augmented training set during training.

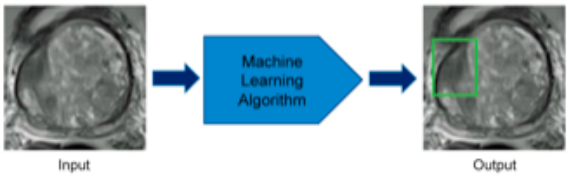

Figure 3: Input and Output of lesion Detection Algorithm [8]

2.3 Prostate Lesion: Classification

In the preceding sections, we explored how various algorithms can segment the prostate gland in prostate mp-MRI and detect various lesions in these images. It is important to note that not all lesions are cancerous; some are significant (malignant) while others are not (benign), which can lead unnecessary biopsies.

Gleason Grade Group (GGG) have also been used to classify lesions into different grades. Oscar J et al. [21] classified the lesions into four classes GGG0 or benign (57.32% of all lesions), GGG1 (GS 3+3, 17.28%), GGG2 (GS 3+4, 12.70%), and GGG3+ (GS 4+3, 12.70%); therefore, lesions of GGG3 were grouped into a single category to try to balance the classes.

PI-Rads system was established to standardise the scoring of lesion with PI-RADS scoring system. Litjens et al. [29] developed a computer-aided detection (CAD) system that utilized a random forest algorithm to evaluate prostate lesions in terms of their potential for malignancy. By combining the machine learning generated scores and the radiologist-provided PI-RADS scores on a dataset of 107 patients, they found that the overall area under the curve (AUC) was higher than either the ML generated scores or the PI-RADS scores [29]. Similarly, Wang, J. et al. [30] also concluded that using a support vector machine (SVM) algorithm improved the performance of radiologists when using PI-RADS on their dataset of 54 patients. Schelb et al. [31] obtained a sensitivity/specificity of 0.99/0.24 using a segmentation CNN, a performance that they found comparable to radiologist-derived PI- RADS scores.

In conclusion, various methods have been developed to classify lesions in the prostate, many of which are based on machine learning and deep learning. It may be beneficial to detect lesions without classifying them, allowing for more input from radiologists. However, classifying the lesions can provide radiologists with a machine generated opinion to consider before making a diagnosis. The precision of these methods suggests they are reliable and could potentially lead to more accurate diagnoses than those made by radiologists currently.

3. Proposed System

3.1 Objectives

In the medical field, AI has the potential to provide accurate diagnosis even better than current doctors. Algorithms can take in more information than usual doctors and can detect detailed features that the human eye cannot see. Although AI has not yet reached a point where it can replace a doctor's diagnosis, it has the potential to do so within the next few years. This raises questions about whether patients would prefer an algorithm or a doctor for their diagnosis. Scientists are now looking into ways of creating a computer-aided diagnosis software that combines human intelligence with machine intelligence to produce faster and more accurate diagnoses of prostate cancer using non-invasive techniques such as MRI images.

The Goal is not to take over the doctor's role but provide them insights and visualisations that would make the diagnoses easier, faster, and accurate.

The primary objectives are as follows:

1. Build CAD algorithm to perform prostate segmentation, lesion detection and lesion classification. The algorithm is to be designed to perform all three tasks together in a single research.
2. Provide doctors insights and visualisations that would make the diagnoses easier, faster, and accurate.
3. To make the model work well, training data must be meticulously annotated to ensure robustness.

3.2 Materials and Methods

To construct, train and evaluate any machine learning model, a valid dataset and a well-defined architecture are essential. This chapter will provide an overview of the datasets used to create the various models, as well as the architecture of each model.

3.2.1 MRI Imaging Techniques

Magnetic Resonance Imaging (MRI) is a powerful imaging technique used to detect and diagnose prostate cancer. MRI uses a combination of radio waves and strong magnetic fields to create detailed images of the body's internal structures. It is particularly useful for detecting prostate cancer because it can provide detailed images of the prostate gland and surrounding tissues.

The most used MRI techniques for prostate cancer detection are T1-weighted (T1W), T2-weighted (T2W), Apparent Diffusion Coefficient (ADC), Diffusion Weighted Imaging (DWI), and K-trans. Each technique has its own advantages and disadvantages, so it is important to understand how each works to choose the best technique for a particular patient.

T1W imaging is the most used MRI technique for prostate cancer detection. It produces high-resolution images that can be used to identify tumors, as well as other abnormalities in the prostate gland. The main advantage of T1W imaging is that it can detect small tumors that may not be visible on other imaging techniques. However, it does not provide information about the tumor's aggressiveness or stage of development.

T2W imaging is another common MRI technique used for prostate cancer detection. It produces images with higher contrast than T1W imaging, which makes it easier to identify tumors and other abnormalities in the prostate gland. The main disadvantage of T2W imaging is that it cannot detect small tumors as well as T1W imaging can.

ADC imaging is a newer MRI technique that uses diffusion-weighted sequences to measure water diffusion within tissues, which can help differentiate between benign and malignant lesions in the prostate gland. ADC images are more sensitive than T1W or T2W images, but they are also more difficult to interpret due to their low contrast resolution.

DWI is an advanced MRI technique that uses multiple sequences with different diffusion sensitivities to measure water diffusion within tissues, which can help differentiate between benign and malignant lesions in the prostate gland. DWI images are more sensitive than ADC images, but they also require more expertise to interpret due to their complex nature.

K-trans is an advanced MRI technique that uses dynamic contrast enhancement sequences to measure tissue perfusion within tissues, which can help differentiate between benign and malignant lesions in the prostate gland. K-trans images are more sensitive than DWI or ADC images, but they also require more expertise to interpret due to their complex nature.

In conclusion, MRI techniques such as T1W, T2W, ADC, DWI, and K-trans are all useful tools for detecting and diagnosing prostate cancer. Each technique has its own advantages and disadvantages depending on the patient's individual needs; therefore, it is important for physicians to understand how each works to choose the best technique for a particular patient's situation

3.2.2 DATASETS

This section contains information about the MRI datasets that were used to train,validate and test the ML models.

I. PROSTATE SEGMENTATION

For training the model for prostate segmentation the dataset used was part of a challenge

In 2012, the Medical Image Computing and Computer Assisted Intervention Society (MICCAI) organised the PROMISE12 [25] challenge with the aim of comparing interactive and (semi)-automatic segmentation algorithms for MRI of the prostate. This dataset is widely recognised in the scientific community as a benchmark for prostate MR image segmentation and consists of 50 training cases with corresponding manual masks and 30 testing cases from different centres and MR scanner vendors (see table 2.1). Each case has between 15 to 54 transverse T2W prostate MR images with mean of 22.7. Each slice is of shape 320x320 or 512x512. The labels of the testing cases are not provided, as they are used to evaluate the challenge algorithms.

II. Lesion Detection & Classification

For training the model to train of detecting the lesions and classifying the lesion into Ca & non-Ca we use dataset from another online challenge. The dataset of the ProstateX challenge [19] was used. This challenge was the live continuation of the offline ProstateX Challenge ("SPIE-AAPM-NCI Prostate MR Classification Challenge") that was held in conjunction with the 2017 SPIE Medical Imaging Symposium [19].

The ProstateX dataset consists of 204 mp-MRIs, each from a different patient. Furthermore, 140 additional mp-MRIs are provided as part of the challenge set. These mp-MRIs include T2-weighted, diffusion-weighted with b-values b50, b400, and b800 s/mm2, an apparent diffusion coefficient map (calculated from the b-values), and K-trans (computed from dynamic contrast-enhanced -DCE- T1-weighted series). For each patient, we have 18 to 27 slices with a mean of 20.42. Each slice is of shape 320x320, 384x384, or 640x640. The 204 dataset of patient is part of training and the remaining 140 patients for testing.

4. Architecture

The whole study is divided into two different models. One for prostate segmentation and other for lesion detection and classification. Both the model uses U-Net architecture.

U-Net is a convolutional neural network (CNN) architecture used for medical image segmentation. It was developed by Olaf Ronneberger, Philipp Fischer, and Thomas Brox at the University of Freiburg, Germany, in 2015[5]. The U-Net architecture is based on the Fully Convolutional Network (FCN) and is designed to perform semantic segmentation of medical images. The U-Net architecture consists of a contracting and an expansive path. The contracting path is composed of a series of convolutional layers and max-pooling layers, while the expansive path is composed of a series of convolutional layers and up-sampling layers. The contracting path is used to capture the context of the input image, while the expansive path is used to recover the spatial information lost during the down-sampling process. The U-Net architecture also includes skip connections between the encoder and decoder. These skip connections allow the network to learn more complex features by combining features from different levels of the network.

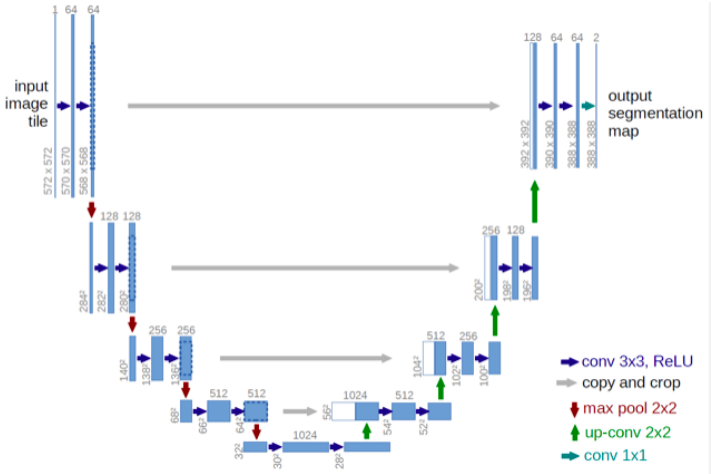

Figure 4: U-Net architecture

4.1 Pre-Processing

I. Prostate Segmentation

The PROMISE12 Challenge involves images and their corresponding masks. As mentioned earlier, the shapes of the slices and images are different. To ensure that all shapes are the same size, we have chosen to reshape them to a size of 256x256. This size is deemed to be the perfect size for reshaping the images.

After the reshaping, to make the images more robust an image deionizing algorithm is applied to smooth the images to preserve the sharp boundaries. The last step in preprocessing this model is to apply normalization, so that we can subtract the dataset's mean and divide it by its standard deviation.

A. Structure

The PROMISE 12 Dataset consists of 50 patients, where 15 % is given to testing and 85 % to training & validation i.e., 8 patients for testing and 42 patients for training and validation. 5 patients are used for validation, so only 36 patients are kept for training.

The structure of this model is to take T2-W images as input and produce a segmentate of the prostate in black and white, white represents the prostate gland and black represents background. The architecture is based on U-Net architecture, and it is described as below:

1. The first convolutional layer has 8 channels.
2. The network has a depth of 5.
3. Zero padding and Rectified Linear Unit (ReLU) are used for the convolutions.
4. Sigmoid is used as the activation function for the last layer.
5. Variance scaling is used for kernel initialization.
6. Batch normalization is applied after each convolutional layer.
7. A dropout of 50% is used between convolutional layers to regularize the network and avoid overfitting.
8. Residual connections are used within the convolutional blocks.

II. Lesion Detection & Classification

The ProstateX challenge provided a variety of MRI modalities, including T2-W (3 axes), PDW, DCE (K-trans), and DWI (ADC map and B-values images). Alex Hamilton significantly impacted the pre-processing of ProstateX. This process is vital and requires a significant amount of time, so we utilized the codes and methodology provided in [4] to streamline it.

In this study, the axial T2-W, K-trans, B-val, and ADC volumes were selected for analysis. PDW images were not included because they are not commonly used in the diagnosis of prostate cancer. All the images were in DICOM format except for the K-trans images, which were in mhd and raw formats. To ensure that all images were in the same format, we converted them to the NIFTI format for processing. This format is ideal for loading 3D volumes as a single file and can be easily accessed using Python libraries.

Voxel spacing refers to the distance between individual voxels in a 3D image. This distance is usually measured in millimeters and is used to determine the resolution of the image. To ensure consistency, we adjust the voxel spacing of the images so that each image has the same voxel spacing.

The PROSTATEx dataset does not include masks for the lesions, but rather provides coordinates for each lesion. We could use SimpleITK to create the masks from these coordinates, however, this method is not very accurate. Instead, we use masks that have been manually created by experienced radiologists [44][45]. These masks provide a more reliable option than generating the masks with SimpleITK.

Similarly, when resampling the voxel spacing of MRI images, we also resample the provided masks according to [44][45]. Other preprocessing steps include registering the masks and other MRI modalities to the corresponding T2-W image for each patient, normalizing the MRI modalities, cropping the masks and images to a size of 128x128 pixels around the prostate zone, stacking the images and masks in a NumPy array, and performing one-hot encoding on the masks.

In this study only preprocessing of the ProstateX dataset could be achieved, the final lesion detection and classification model will be discussed in future work.

5. Result

The steps taken to preprocess the data and the architecture used to obtain the results have already been discussed in the sections on preprocessing and architecture. The graph below displays the validation and training loss and accuracy.

The soft Dice Loss function was used to track the performance. Each epoch in my system took approximately 50 minutes to run, so for the test run, epoch 2 was used, while epoch 10 was used for the final result. ImageDataGenertaor was utilized for data augmentation to increase the number of training cases and improve accuracy. Figures 5, 6, and 7 show that the training loss decreases with each epoch. However, the graph in figure 7 for validation lss exhibits strange behavior, with a rapid increase after the 4th epoch and a drastic drop after the 5th epoch. The exact reason for this strange behaviour is unknown.

Figure 5: Training and Validation Loss, epoch =2

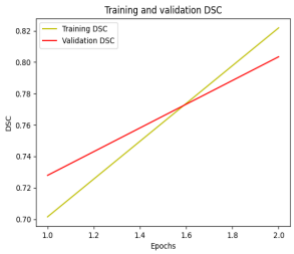

Figure 6: Training and Validation Dice Score, epoch = 2

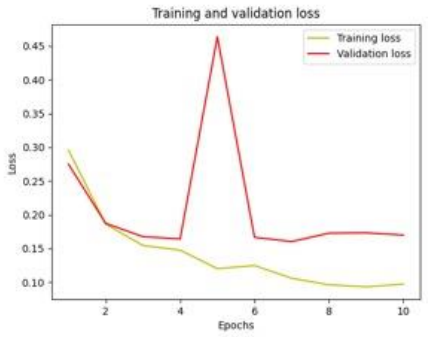

Figure 7: Training and Validation Loss, epoch = 10

Now let us look at the scores achieved on the test data set.

- DSC: 0.8718
- Mean Relative Absolute Volume Difference: 9.42%
- Hausdorff Distance: 8.3

6. Future Work

The goal of this project was to create a comprehensive system for identifying and categorizing prostate lesions, but I only succeeded in creating a segmentation model for the prostate. Additionally, I only could partially complete the preprocessing of the ProstateX data for the second model.

Additional work on the project is to create a complete pipeline to take different mp-MRI modalities and generate a segmentation of lesion and classify into its significance. Additionally, to visualize the lesions, Gradient-Weighted Class Activation Mapping (Grad-CAM) have been considered to be used in future. Grad-CAM generates a map that shows important regions in the image based on the predicted concept by using the gradients flowing into the final convolutional layer of a network that predicts the target concept.

Deep learning has the potential to replace doctor's diagnoses in the future, but I believe that the use of Computer-Aided Diagnosis (CAD) can provide doctors with insights to help them detect lesions more accurately. While I think doctors' advice is still necessary and we cannot solely rely on the accuracy of machines, this is also an ethical issue as it involves the health of a living being.

To improve accuracy, we could experiment with different image smoothing algorithms and fine-tune the model by adjusting the dropout rate and learning rate

7. Conclusion

The goal of this project was to utilize neural networks and deep learning techniques to assist doctors in accurately identifying prostate cancer in its early stages. The tasks involved in detecting prostate cancer included segmenting the prostate, detecting lesions, and classifying them. Ultimately, only prostate segmentation was successfully completed, along with the preprocessing of ProstateX data. The Dice score for prostate segmentation was 87.1%.

8. References

[1] Rundo, L.; Militello, C.; Russo, G.; Garufi, A.; Vitabile, S.; Gilardi, M.C.; Mauri, G. Automated prostate gland segmentation based on an unsupervised fuzzy C-means clustering technique using multispectral T1w and T2w MR imaging. Information 2017, 8, 49. [CrossRef]

[2] Tian, Z.; Liu, L.; Zhang, Z.; Fei, B. PSNet: Prostate segmentation on MRI based on a convolutional neural network. J. Med. Imaging 2018, 5, 021208. [CrossRef]

[3] Karimi, D.; Samei, G.; Kesch, C.; Nir, G.; Salcudean, S.E. Prostate segmentation in MRI using a convolutional neural network architecture and training strategy based on statistical shape models. Int. J. Comput. Assist. Radiol. Surg. 2018. [CrossRef] [PubMed]

[4] Bardis, M.D.; Houshyar, R.; Chang, P.D.; Ushinsky, A.; Glavis-Bloom, J.; Chahine, C.; Bui, T.-L.; Rupasinghe, M.; Filippi, C.G.; Chow, D.S. Applications of Artificial Intelligence to Prostate Multiparametric MRI (mpMRI): Current and Emerging Trends. Cancers 2020, 12, 1204. [CrossRef]

[5] Ronneberger, O.; Fischer, P.; Brox, T. U-net: Convolutional networks for biomedical image segmentation. In Proceedings of the 2015 International Conference on Medical Image Computing and Computer-Assisted Intervention, Munich, Germany, 5–9 October 2015; pp. 234–241.

[6] Clark, T.; Wong, A.; Haider, M.A.; Khalvati, F. Fully Deep Convolutional Neural Networks for Segmentation of the Prostate Gland in Diffusion-Weighted MR Images; Springer: Cham, Switzerland, 2017; pp. 97–104.

[7] Zhu, Y.; Wei, R.; Gao, G.; Ding, L.; Zhang, X.; Wang, X.; Zhang, J. Fully automatic segmentation on prostate

[8] MR images based on cascaded fully convolution network. J. Magn. Reson. Imaging 2018, 49, 1149–1156. [CrossRef]

[9] Zhu, Q.; Du, B.; Turkbey, B.; Choyke, P.L.; Yan, P. Deeply supervised CNN for prostate segmentation. In Proceedings of the 2017 International Joint Conference on Neural Networks (IJCNN), Anchorage, AK, USA, 14–19 May 2017; pp. 178–184.

[10] Milletari, F.; Navab, N.; Ahmadi, S.-A. V-net: Fully convolutional neural networks for volumetric medical image segmentation. In Proceedings of the 2016 Fourth International Conference on 3D Vision (3DV), Stanford, CA, USA, 25–28 October 2016; pp. 565–571.

[11] Wang, B.; Lei, Y.; Tian, S.; Wang, T.; Liu, Y.; Patel, P.; Jani, A.B.; Mao, H.; Curran, W.J.; Liu, T.; et al. Deeply supervised 3D fully convolutional networks with group dilated convolution for automatic MRI prostate segmentation. Med. Phys. 2019, 46, 1707–1718. [CrossRef]

[12] Cheng, R.; Roth, H.R.; Lu, L.; Wang, S.; Turkbey, B.; Gandler, W.; McCreedy, E.S.; Agarwal, H.K.; Choyke, P.; Summers, R.M. Active appearance model and deep learning for more accurate prostate segmentation on MRI. In Proceedings of the Medical Imaging 2016:

Image Processing, San Diego, CA, USA, 27 February–3 March 2016; p. 97842I.

[13] Lay, N.; Tsehay, Y.; Greer, M.D.; Turkbey, B.; Kwak, J.T.; Choyke, P.L.; Pinto, P.; Wood, B.J.; Summers, R.M. Detection of prostate cancer in multiparametric MRI using random forest with instance weighting. J. Med. Imaging (Bellingham) 2017, 4, 024506. [CrossRef] [PubMed]

[14] Xu, H.; Baxter, J.S.; Akin, O.; Cantor-Rivera, D. Prostate cancer detection using residual networks. Int. J. Comput. Assist. Radiol. Surg. 2019, 14, 1647–1650. [CrossRef]

[15] He, K.; Zhang, X.; Ren, S.; Sun, J. Deep residual learning for image recognition. In Proceedings of the 2016 IEEE Conference on Computer Vision and Pattern Recognition, Las vegas, NV, USA, 26 June–1 July 2016; pp. 770–778.

[16] Tsehay, Y.K.; Lay, N.S.; Roth, H.R.; Wang, X.; Kwak, J.T.; Turkbey, B.I.; Pinto, P.A.; Wood, B.J.; Summers, R.M. Convolutional neural network based deep-learning architecture for prostate cancer detection on multiparametric magnetic resonance images. In Medical Imaging 2017: Computer-Aided Diagnosis; SPIE: Bellingham, WA, USA, 2017; p. 1013405. [CrossRef]

[17] Le, M. H. et al. Automated diagnosis of prostate cancer in multi-parametric mri based on multimodal convolutional neural networks. Phys. Medicine & Biol. 62, 6497 (2017).

[18] Liu, S., Zheng, H., Feng, Y. & Li, W. Prostate cancer diagnosis using deep learning with 3d multiparametric mri. In Medical Imaging 2017: Computer-Aided Diagnosis, vol. 10134, 1013428 (International Society for Optics and Photonics, 2017).

[19] Simonyan, K. & Zisserman, A. Very deep convolutional networks for large-scale image recognition. arXiv preprint arXiv:1409.1556 (2014).

[20] SPIE-AAPM-NCI PROSTATEx Challenges. url: [CrossRef] (visited on 05/14/2021).

[21] Mehrtash, A. et al. Classification of clinical significance of mri prostate findings using 3d convolutional neural networks. In Medical Imaging 2017: Computer-Aided Diagnosis, vol. 10134, 101342A (International Society for Optics and Photonics, 2017).

[22] Pellicer-Valero, Oscar J., et al. “Deep Learning for Fully Automatic Detection, Segmentation, and Gleason Grade Estimation of Prostate Cancer in Multiparametric Magnetic Resonance Images.” Scientific Reports, vol. 12, no. 1, Feb. 2022. Crossref, [CrossRef]

[23] Liu, X.; Langer, D.L.; Haider, M.A.; Yang, Y.; Wernick, M.N.; Yetik, I.S. Prostate cancer segmentation with simultaneous estimation of Markov random field parameters and class. IEEE Trans. Med. Imaging 2009, 28, 906–915. [CrossRef]

[24] Kohl, S.; Bonekamp, D.; Schlemmer, H.-P.; Yaqubi, K.; Hohenfellner, M.; Hadaschik, B.; Radtke, J.-P.; Maier-Hein, K. Adversarial networks for the detection of aggressive prostate cancer. ArXiv 2017, arXiv:1702.08014.

[25] Dai, Z.; Carver, E.; Liu, C.; Lee, J.; Feldman, A.; Zong, W.; Pantelic, M.; Elshaikh, M.; Wen, N. Segmentation of the Prostatic Gland and the Intraprostatic Lesions on Multiparametic MRI Using Mask-RCNN. ArXiv 2019, arXiv:1904.02575.

[26] Home - PROMISE12 - Grand Challenge. url: [CrossRef]

[27] Yoo, Sunghwan, et al. “Prostate Cancer Detection Using Deep Convolutional Neural Networks.” Scientific Reports, vol. 9, no. 1, Dec. 2019 [CrossRef].

[28] Ishioka, J. et al. Mp20-10 deep learning with a convolutional neural network algorithm for fully automated detection of prostate cancer using pre-biopsy mri. The J. Urol. 199, e256 (2018).

[29] Wang, X. et al. Searching for prostate cancer by fully automated magnetic resonance imaging classification: deep learning versus non-deep learning. Sci. reports 7, 15415 (2017).

[30] Litjens, G.J.; Barentsz, J.O.; Karssemeijer, N.; Huisman, H.J. Clinical evaluation of a computer-aided diagnosis system for determining cancer aggressiveness in prostate MRI. Eur. Radiol. 2015, 25, 3187–3199. [CrossRef]

[31] Wang, J.; Wu, C.-J.; Bao, M.-L.; Zhang, J.; Wang, X.-N.; Zhang, Y.-D. Machine learning-based analysis of MR radiomics can help to improve the diagnostic performance of PI-RADS v2 in clinically relevant prostate cancer. Eur. Radiol. 2017, 27, 4082–4090. [CrossRef] [PubMed]

[32] Patrick Schelb, Xianfeng Wang, Jan Philipp Radtke, Manuel Wiesenfarth, Philipp Kickingereder, Al- brecht Stenzinger, Markus Hohenfellner, Heinz Peter Schlemmer, Klaus H. Maier-Hein, and David Bonekamp. Simulated clinical deployment of fully automatic deep learning for clinical prostate MRI assessment. Eur. Radiol., pages 1–12, aug 2020. [CrossRef]

[33] American Cancer Society. Facts & Figures 2022. American Cancer Society. Atlanta, Ga. 2022.

[34] PDQ® Adult Treatment Editorial Board. PDQ Prostate Cancer Treatment. Bethesda, MD: National Cancer Institute. Updated <12/07/2022> [PMID: 26389353] [CrossRef]

[35] Prostate Cancer Foundation. "Prostate Cancer Basics: Symptoms, Causes, Treatment, Side Effects." Prostate Cancer Foundation, 18 Aug. 2021, [CrossRef]

[36] Holtappels R, Schader SI, Oettel O, Podlech J, Seckert CK, Reddehase MJ, Lemmermann NAW. Insufficient Antigen Presentation Due to Viral Immune Evasion Explains Lethal Cytomegalovirus Organ Disease After Allogeneic Hematopoietic Cell Transplantation. Front Cell Infect Microbiol. 2020 Apr 15; 10:157 [CrossRef]. PMID: 32351904; PMCID: PMC7174590.

[37] "PI-RADS." American College of Radiology, [CrossRef].

[38] Canadian Cancer Society. The prostate [CrossRef] (visited on 05/12/2021).

[39] Net Convolutional Networks for Biomedical Image Segmentation [CrossRef].

[40] VGG in TensorFlow, [CrossRef].